Photodiagnosis and Photodynamic Therapy 27 (2019) 79–84

Contents lists available at ScienceDirect

Photodiagnosis and Photodynamic Therapy

journal homepage: www.elsevier.com/locate/pdpdt

Effects of low-dose ALA-PDT on fibroblast photoaging induced by UVA irradiation and the underlying mechanisms

Jinyi Chen[a,1], Jiefu Luo[a,1], Yang Tan[a], Mei Wang[b], Zhihua Liu[c], Tao Yang[a], Xia lei[a,*]

[a] Department of Dermatology, Daping Hospital, The Army Medical University, Chongqing, 400042, China
[b] Key Laboratory of Biorheological Science and Technology, Ministry of Education; Chongqing University, Chongqing, 400044, China
[c] Department of Stomatology, Daping Hospital, The Army Medical University, Chongqing, 400042, China

ARTICLE INFO

Keywords:
ALA-PDT
NF-E2-related factor 2 (Nrf2)
Photoaging
HDFs

ABSTRACT

Objectives: To investigate the effects of low-dose aminolevulinic acid photodynamic therapy (ALA-PDT) on photoaging in human dermal fibroblasts (HDFs) and to explore the mechanism of Nuclear factor erythroid 2-related factor 2(Nrf2)-mediated photorejuvenation in vitro.

Methods: A photoaging model was established through repeated exposure of HDFs to UVA. Total superoxide dismutase (SOD) expression was detected by a SOD activity assay. Nrf2 was knocked down through adenovirus infection, and successful knockdown was confirmed by Western blot analysis and quantitative polymerase chain reaction.

Results: Sustained exposure to UVA induced photoaging in HDFs. Total SOD activity was significantly increased by low-dose aminolevulinic acid (ALA)-PDT. Upon application of low doses of ALA-PDT to photoaging HDFs, Nrf2 was translocated to the nucleus; in addition, the expression of Nrf2, transforming growth factor-β1 (TGF-β1), type I and III collagen (COL1 and COL3), heme oxygenase 1 (HO-1), and p-ERK was increased, while the expression of matrix metalloproteinase 9 (MMP-9) was decreased. However, after Nrf2 was knocked down in HDFs, the expression of TGF-β1, COL1, COL3, and HO-1 was significantly decreased, while the expression of MMP-9 was increased.

Conclusion: This study revealed that low-dose ALA-PDT decreases UVA-mediated photoaging through an Nrf2-mediated antioxidant effect.

1. Introduction

Skin aging includes both intrinsic and extrinsic skin aging [1]. Extrinsic aging may be associated with exposure to ultraviolet radiation, cold, harmful chemicals, nicotine use, lifestyle, diet, and other factors [2]. Approximately 90%–99% of the longwave ultraviolet rays in sunlight can reach the earth's surface, penetrate human skin dermal tissue, reduce the synthesis of collagen and other extracellular matrix proteins and cause abnormal degradation, thus leading to changes in the quality and quantity of dermal matrix and causing skin photoaging [3]. Skin photoaging not only ages the skin and affects human health, aesthetics, psychology, and quality of life [4] but is also closely associated with many clinical skin diseases, such as solar keratosis, PUVA lentigines, and basal cell carcinoma. Currently, photoaging prevention and treatment agents include antiaging products and sunscreen. However, many studies have reported that photodynamic therapy (PDT) for photoaging has achieved good clinical efficacy. PDT is a treatment featuring a redox reaction produced by the action of photosensitizers, oxygen and specific wavelengths of light [5]. A growing number of studies have shown that low-dose ALA-PDT promotes cell proliferation, accelerates skin healing, and heals photoaging [6,7]; the mechanisms may be associated with increases in collagen in the dermis and reductions in solar elastosis that improve the texture and appearance of the skin [8]. The European Dermatology Forum Guidelines published in 2015 classified PDT skin rejuvenation as a grade A recommendation [9]. Previous studies have shown that the ultimate oxidative stress-related effects of PDT differ with different light sources and photosensitizers, sites of action, cells, and other factors. Nuclear factor erythroid 2-related factor 2 (Nrf2) is a key factor in the oxidative stress response that regulates the expression of downstream antioxidant proteins and growth factors [10,11] and plays an important role in skin phototherapy and cell defense.

The transcription factor Nrf2 was discovered in 1994 [12]. Nrf2

* Corresponding author.
E-mail address: leixia1979@sina.com (X. lei).
[1] These authors contributed equally to this work.

https://doi.org/10.1016/j.pdpdt.2019.05.006
Received 16 February 2019; Received in revised form 22 April 2019; Accepted 6 May 2019
Available online 07 May 2019

contains a basic leucine zipper (bZIP) and is currently considered to be the most active transcription factor belonging to the cap 'n' collar (CNC) family. Nrf2 activity is regulated by the cytoplasmic binding protein Keap1. Once stimulated by internal free radicals or chemicals, Nrf2 detaches from the Keap1 binding site and binds to the protein Maf. Activated Nrf2 translocates into the nucleus and binds to the antioxidant response element (ARE) [13], regulating the transcription and translation of a series of detoxification and antioxidant genes [10]. Nrf2 plays a very important role in cell defense and healing from photoaging. However, the role of Nrf2 in the treatment of photoaging with low-dose PDT remains unclear and is worthy of further study. This study revealed that low-dose ALA-PDT-induced activation of Nrf2 nuclear transcription is conducive to collagen proliferation and the reversal of photoaging.

2. Materials and methods

2.1. Cell culture

Primary HDFs were obtained from circumcisions in accordance with the approval process of the Ethics Committee at Daping Hospital of Army Medical University (Chongqing, China). The method of fibroblast isolation was based on the previous experience of our department [14]. The HDFs were cultured in DMEM supplemented with 10% fetal bovine serum, 100 U/ml penicillin and 100 μg/ml streptomycin (all from Invitrogen, USA) in an incubator at 37 °C under 5% CO_2 with 95% relative humidity. Cells in the logarithmic phase in the fourth through sixth generations were selected for the following experiments.

2.2. Establishment of the photoaging model

The ultraviolet A (UVA) source used in the experiment was an SS07 UV phototherapy instrument (Sigma, Shanghai, China). The samples were uniformly exposed to UVA radiation at a distance of 4 cm. Before UV irradiation, the cells were washed twice with phosphate-buffered saline (PBS) and covered with a thin layer of PBS. Subsequently, the cells were exposed to various intensities of UVA radiation (0, 5, 10, and 20 J/cm^2) for five days and then cultured in fresh ordinary DMEM. Ultimately, 10 J/cm^2 was selected for the HDF photoaging model and used for all experiments.

2.3. PDT

Cells were randomly divided into five groups: the UVA group (photoaging group, 10 J/cm^2), the aminolevulinic acid (ALA) group (0.1 mmol/L ALA without red light irradiation), the red light group (21 J/cm^2 red light without ALA), the ALA-PDT1 group (0.1 mmol/L ALA with 21 J/cm^2 red light), and the ALA-PDT2 group (1.0 mmol/L ALA with 21 J/cm^2 red light). PDT was performed for 2 h after 12 h of UVA irradiation. The red light source was a 630 nm LED (Omnibus, UK), and the energy of the red light radiation was 21 J/cm^2.

2.3.1. Senescence-Associated ß-Galactosidase (SA-ß-Gal) staining

HDFs were exposed to UVA radiation at 0, 5, 10, and 20 J/cm^2 per day for 5 days and then collected for SA-β-gal staining (Beyotime, Nanjing, China). At 24 h after the last irradiation, SA-β-gal staining was performed according to the manufacturer's instructions. After incubation overnight, the cells were washed with PBS. Three high-magnification fields were randomly selected, and the number of positive cells per 400 cells was counted in each of the randomly chosen microscopic fields. The percentage of positive cells was calculated according to the following equation: positive cell rate (%) = stained cell number/total cell number × 100%.

2.3.2. Real-Time Cell Analyzer (RTCA) system

UV-induced toxicity was measured using an RTCA system (Roche Applied Sciences, USA). After trypsin digestion, the cells were seeded at a density of 1×10^4 cells per well into a sensor E-plate (Roche Applied Sciences, USA), and 200 μL of medium was added to each well. The cells were randomly divided into 4 groups and treated with 0, 5, 10, or 20 J/cm^2 UVA for 24 h. Three replicates were analyzed for each group. After incubation at room temperature for 10 min, the E-plate was loaded into the RTCA system in a cell culture incubator at 5% CO_2 and 37 °C, and real-time measurement of cell status was initiated. The RTCA system recorded the cell index (CI) for each well automatically every 5 min for 5 consecutive days.

2.3.3. SOD activity assay

HDFs (3×10^5) were seeded into different groups of 100mm dishes and grown for 24 h; the cells were divided into groups according to the PDT regimen they received. According to the instructions provided with the SOD Assay Kit (Beyotime, Nanjing, China), the cell suspensions were treated with working buffers for 30 min at 37 °C. The optical density (OD) values were then detected at 450 nm, and the total SOD activity was calculated for each dish.

2.4. Western blot analysis

HDFs were harvested 12 h after ALA-PDT, and nuclear and cytoplasmic protein lysates were prepared. The protein concentrations were measured with a BCA Protein Assay Kit (Beyotime, Nanjing, China). Equal amounts of protein (30 μg) were loaded into each lane, and the proteins were separated by 10% sodium dodecyl sulfate polyacrylamide gel electrophoresis (SDS-PAGE). After the proteins were transferred onto polyvinylidene difluoride membranes, the membranes were blocked and incubated with primary antibodies at 4 °C overnight. The primary antibodies included anti-Nrf2, anti-COL1, anti-COL3, anti-MMP-9, anti-caspase-3, and anti-TGF-β antibodies from Abcam (USA); an anti-β-actin antibody from Bioworld (USA); an anti-HO-1 antibody from Enzo Life Sciences; and an anti-PARP antibody from CST (USA). After incubation with the secondary antibody (goat anti-rabbit), the membranes were treated with an enhanced chemiluminescence reagent mixture (Thermo, USA) for 5 min and imaged on a Vilber Lourmat (Fusion FX5 system, China).

2.5. Adenovirus infection

Nrf2 expression in HDFs was knocked down by adenovirus infection (De Novo Biotechnology, Ltd., Chongqing, China). The HDFs (3×10^5 cells/well) were cultured to 40–60% confluence in 100-mm dishes before UVA irradiation. The day after the photoaging cell model was successfully established, adenoviral vectors expressing red fluorescent protein (RFP) (Ad-RFP, Ad-Vector) and vectors expressing Nrf2 (Ad-siNrf2) were added to cells in the presence of polybrene (Sigma, 8 mg/ml) at a series of multiplicities of infection (MOIs), i.e., 2.5, 5, 10, and 20. Fluorescence intensity analysis and immunoblot analysis were used to confirm the knockdown efficiency of Nrf2. Thirty-six hours after adenovirus infection, low-dose (0.1 mmol/L) ALA-PDT was administered, and the total proteins were prepared for Western blot analysis the next day.

2.6. Quantitative Polymerase Chain Reaction (qPCR)

HDFs were harvested 24 h after adenovirus infection, and total RNA was isolated using TRIzol reagent according to the manufacturer's instructions (Life, USA). Then, the RNA was reverse transcribed into cDNA with SuperScript II reverse transcriptase (Roche, USA), and qPCR was performed with SYBR Ex Taq according to the manufacturer's instructions. The primer sequences were as follows: NRF2 forward, 5′-TCAGCGACGGAAAGAGTA-3′; Nrf2 reverse, 5′-TGGGAGTAGTTGGC AGATC-3′; GAPDH forward, 5′−CCTGCACCACCAACTGCTTA-3′; and GAPDH reverse, 5′-AGGCCATGCCAGTGAGCTT-3′. The qPCR data were analyzed with a LightCycler 96 (Roche, USA).

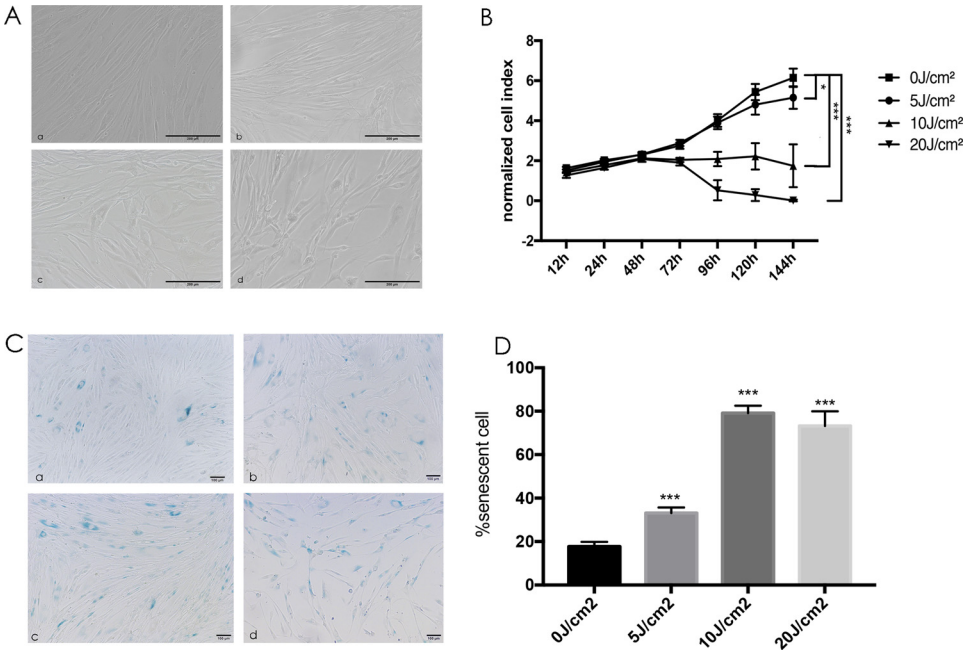

Fig. 1. Establishment of the photoaging model. (A) Morphological changes in HDFs subjected to different doses of UVA radiation. a: UVA 0 J/cm^2, b: UVA 5 J/cm^2, c: UVA 10 J/cm^2, d: UVA 20 J/cm^2. Scale bar = 200 μm. (B) Proliferation of HDFs detected by the RTCA system after exposure to different doses of UVA radiation. The cell index (CI) values are presented as the mean ± SD. $^*p < 0.05$ and $^{***}p < 0.005$ versus the control group. (CD) Senescence-associated β-galactosidase (SA-β-gal) staining. a: UVA 0 J/cm^2, b: UVA 5 J/cm^2, c: UVA 10 J/cm^2, d: UVA 20 J/cm^2. Scale bar = 100 μm. The digitalized results are shown as the mean ± SD. $^{***}p < 0.005$ versus the control group.

2.7. Statistical analyses

All experiments were independently performed with three replicates. The results are presented as the mean ± SD. Statistical differences were analyzed by Student's *t*-test or one-way ANOVA with SPSS Statistics 20.0 (IBM, USA). *P*-values less than 0.05, 0.01, 0.005 or 0.0005 were considered to indicate statistically significant differences.

3. Results

3.1. Establishment of the skin photoaging model

3.1.1. HDF morphology was changed by UVA irradiation

Through an inverted microscope, it was observed that HDFs adhered to the plates and grew into fusiform shapes, and pseudopods gradually emerged. After UVA irradiation, the cells became flat, and degranulation occurred, especially after 10 J/cm^2 UVA. In addition, cell shrinkage was observed through the inverted microscope, and some cells were observed to float in the medium. With increasing UVA intensity, especially when the UVA dose reached 20 J/cm^2, apoptosis began to occur (Fig. 1A).

3.1.2. Effects of UVA on HDF proliferation

Upon analysis of the resistivity of the bottom of the E-plate, there were no significant differences in proliferation among the groups treated with different doses of UVA (0, 5, 10, and 20 J/cm^2)before 48 h. After 72 h, there were drastic differences in CI among the groups, it still tends to be increasing in groups with 0 and 5 J/cm^2 while it stays stagnant in the 10 and 20 J/cm^2 groups. At 144 h, the CIs of the UVA-treated groups were significantly different from the CI of the control group. When the UVA dose was 20 J/cm^2, cell proliferation was significantly inhibited, and the proliferation curve was negatively affected (Fig. 1B).

3.1.3. UVA increased the proportion of β-gal-positive cells

After HDFs were irradiated with different doses of UVA for 5 days, cell senescence was examined using SA-β-gal cytochemical staining. The results showed that UVA increased the proportion of senescent cells in an intensity-dependent manner. When the UVA dose increased from 5 to 20 J/cm^2, the percentage of SA-β-gal-positive cells became significantly different from that of the control group ($^{***}p < 0.005$). In addition, when the UVA dose reached 20 J/cm^2, the cells began shrinking into clumps, and apoptosis occurred, while other cells were stained blue (Fig. 1C and D).

3.2. ALA-PDT enhanced the total SOD activity in photoaging HDFs

As shown in Fig. 2, the total SOD activity in photoaging HDFs was significantly increased by ALA-PDT. In particular, there was no significant difference in SOD activity between the ALA group and the control group, while total SOD activity was clearly higher in both the red light group and the ALA-PDT group ($^*p < 0.05$) than in the control group. In addition, the SOD activity in the ALA-PDT1 group was 0.18-fold higher than that in the ALA-PDT2 group. Taken together, these findings suggest that ALA-PDT could improve SOD activity in photoaging HDFs, especially those in the low-dose group (ALA-PDT1).

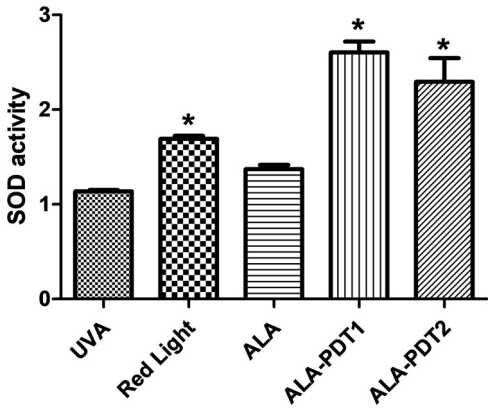

Fig. 2. ALA-PDT enhanced total SOD activity. HDFs were randomly divided into five groups: the UVA group (photoaging group, 10 J/cm^2), the ALA group (0.1 mmol/L ALA without red light irradiation), the red light group (21 J/cm^2 red light without ALA), the ALA-PDT1 group (0.1 mmol/L ALA with 21 J/cm^2 red light), and the ALA-PDT2 group (1.0 mmol/L ALA with 21 J/cm^2 red light). Total SOD activity was calculated by measuring OD values using a spectrophotometer (mean ± SD). $^*p < 0.05$ versus control group.

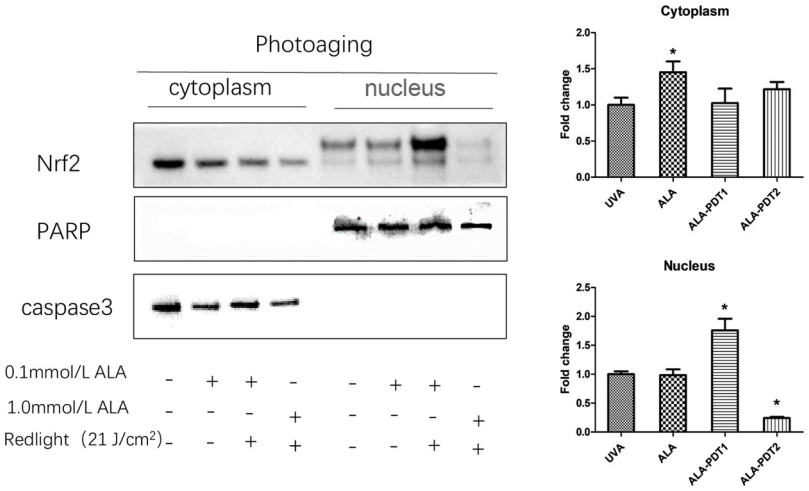

Fig. 3. ALA-PDT enhanced the nuclear translocation of Nrf2 in HDFs. After treatment of photoaging HDFs with UVA (10 J/cm^2), red light (21 J/cm^2), or ALA (0.1 mmol/L or 1.0 mmol/L) for 12 h, the HDFs were collected for Western blot analysis. Cytosolic and nuclear proteins were isolated, and Nrf2 protein levels were determined. Caspase-3 (a cytosolic marker) and PARP (a nuclear marker) were used as isolation controls to demonstrate successful cytosolic and nuclear fractionation and as equal loading controls. *$p <$ 0.05 versus the UVA and ALA-PDT1 groups in the cytoplasm or versus the other groups in the nucleus.

3.3. The low dose of ALA-PDT enhanced the nuclear translocation of Nrf2 in HDFs

Studies have shown that Nrf2 binds to Keap1 under physiological conditions to form a dimer. After stimulation, Nrf2 detaches from the Keap1 binding site and translocates into the nucleus to participate in antioxidant activities. To further support this mechanism, we used a nucleoprotein isolation kit to detect the expression of Nrf2 in the nucleus and cytoplasm after ALA-PDT of photoaging cells. As shown in Fig. 3, nuclear expression of Nrf2 was increased most significantly in the ALA-PDT1 group (0.1 mmol/L ALA and 21 J/cm^2 red light), while the other groups did not show clear increases in nuclear Nrf2 expression, indicating that ALA-PDT1 could stimulate the nuclear translocation of the transcription factor Nrf2.

3.4. Effects of ALA-PDT on the expression of Nrf2 and related proteins in photoaging HDFs

Compared with the control group and the UVA photoaging group, the ALA-PDT1 group (0.1 mmol/L ALA and 21 J/cm^2 red light) showed significant increases in the expression of Nrf2 and related proteins, including TGF-β1, HO-1, COL1, COL3, and p-ERK (among which HO-1, COL1, and COL3 exhibited the greatest increases), and a significant decrease in the expression of MMP-9. In addition, the protein expression of COL1 was slightly increased in the red light group but was still significantly lower than that in the ALA-PDT1 group(Fig. 4). These results indicated that low-dose ALA-PDT could enhance the transcriptional activity of Nrf2 in photoaging HDFs.

3.5. Effects of Nrf2 knockdown on photoaging HDFs

Based on the above results, it was concluded that low-dose ALA-PDT could enhance the antioxidant capacity of HDFs. However, further investigation was needed to determine whether Nrf2 plays a key role. Thus, photoaging HDFs were randomly divided into a UVA group, a low-dose ALA-PDT group infected with Ad-RFP, and a low-dose ALA-PDT group infected with Ad-siNrf2. After the Nrf2 gene was silenced by adenovirus infection of HDFs with Ad-siNrf2, Western blot analysis was performed, and the results showed that the expression of Nrf2, TGF-β1, HO-1, COL1, and COL3 was significantly downregulated in the Ad-siNrf2 group compared to that in the Ad-RFP group, while the expression of MMP-9 was upregulated (Fig. 5).

4. Discussion

Skin photoaging is damage caused by repeated exposure to UV light. UVA light (wavelength, 320–400 nm) can reach the dermis of the skin and is one of the most important environmental factors causing skin photodamage and aging [15], which results in rough skin, thickened skin, sagging skin, wrinkles, pigmentation spots, and other problems. According to reported studies, 80% of skin aging results from photoaging. In our study, upon repeated UVA irradiation of HDFs, we found that cell aging was time dependent and dose dependent. Prolonged UVA irradiation and increasing doses slowed cell proliferation, increased SA-β-gal staining, and even gradually led to apoptosis. With improvements in standards of living, the requirements for beautiful skin are drawing increasing attention as people pursue youthful faces that can resist aging. Current treatments for skin photoaging include acid treatment, laser treatment, botulinum toxin injection, skin filling, surgical treatment, and photodynamic therapies. The demand for therapies is increasing, but fundamental research on treatment principles and mechanisms is still lacking in this field. Thus, research on treatments for skin photoaging and the relevant mechanisms has great social and scientific value.

The principle of ALA-PDT is that in the presence of oxygen, a photosensitizer is activated by light of a suitable wavelength to produce reactive oxygen species (ROS), especially singlet oxygen, which then produce biological effects in target cells. Therefore, singlet oxygen is a core factor in PDT, and ROS play important roles in skin aging [4]. In skin cells, UVA induces high concentrations of ROS, which cause oxidative damage to cell components, e.g., cell membrane macromolecules, proteins, and nucleic acids [16]. Different light sources, photosensitizers, sites of action, cell types, cellular oxygen metabolism levels, and ROS intensities produce different final effects of PDT. In general, high concentrations of ROS give rise to cytotoxicity, inducing apoptosis [17], while low concentrations of ROS can help cells respond to oxidant stress by activating transcription factors, regulating cell proliferation and differentiation, and initiating and maintaining remodeling and regeneration processes [18].

At present, the mechanisms by which low-dose PDT heals photoaging are not clear. On one hand, low-dose PDT may initiate the post injury repair process through photobiomodulation, stimulating the synthesis of type I and III collagens and inducing the secretion of matrix metalloproteinases to remove photodamaged collagens [19,20], thus leading to the reconstruction of extracellular matrix components of the dermis. On the other hand, low-dose ALA-PDT may induce an appropriate amount of oxygen free radicals through photochemical reactions, stimulating intracellular signaling and promoting gene expression and cell proliferation [21]. In this study, it was found that the total SOD activity increased in photoaging HDFs after ALA-PDT. SOD is a major antioxidant enzyme that can remove superoxide anions. High expression of SOD can inhibit cell death and tissue damage caused by

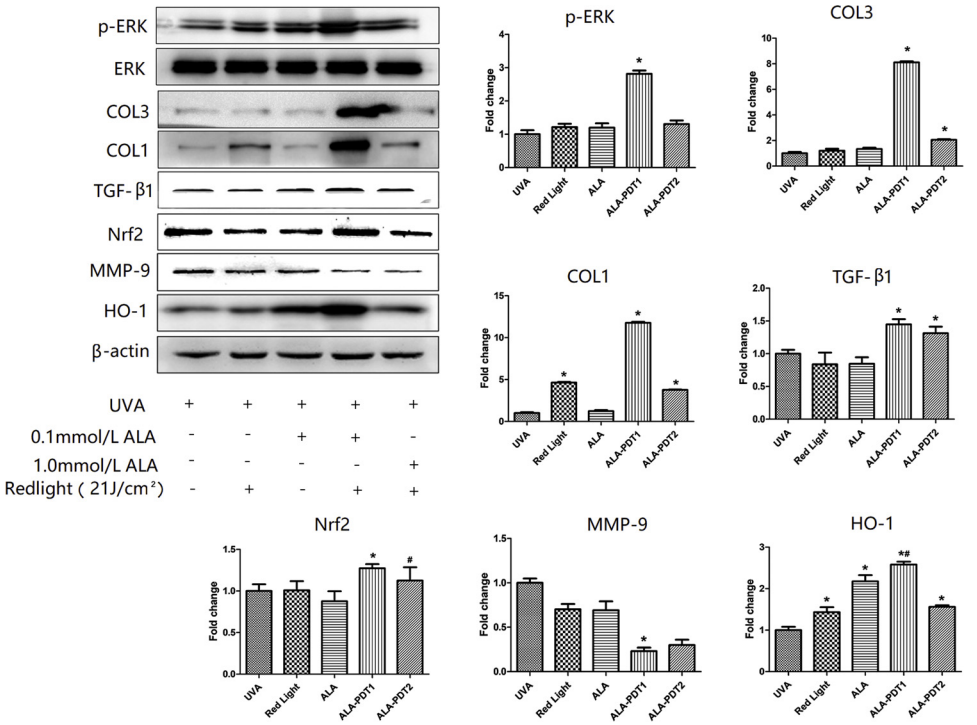

Fig. 4. Effects of ALA-PDT on the expression of Nrf2 and related proteins in photoaging HDFs. HDFs were randomly divided into five groups: the UVA group (photoaging group, 10 J/cm^2), the ALA group (0.1 mmol/L ALA without red light irradiation), the red light group (21 J/cm^2 red light without ALA), the ALA-PDT1 group (0.1 mmol/L ALA with 21 J/cm^2 red light), and the ALA-PDT2 group (1.0 mmol/L ALA with 21 J/cm^2 red light). Low-dose ALA-PDT enhanced the protein expression of Nrf2, TGF-β1, HO-1, COL1, COL3, and p-ERK while lowering MMP-9 expression. For COL1, $*p <$ 0.005 versus the UVA group and the other groups. For COL3, $*p <$ 0.005 versus the UVA group and the other groups. For HO-1, $*p <$ 0.005 versus the UVA group and $\#p <$ 0.005 versus the other groups. For MMP-9, $*p <$ 0.05 versus the UVA group. For Nrf2, $*p <$ 0.05 versus the UVA, red light, and ALA groups, and $\#p <$ 0.05 versus the ALA group. For TGF-β1, $*p <$ 0.01 versus the UVA, red light, and ALA groups. For p-ERK, $*p <$ 0.005 versus the other groups.

oxidative stress; thus, our findings indicate that low-dose ALA-PDT can effectively counteract oxidative stress. It has also been confirmed in human experiments that after photodynamic therapy, the epidermis becomes thinner, the levels of collagens and type I and III procollagens in the superficial dermis increase, and the expression of TGF-β and type II TGF-β receptors, which can stimulate collagen proliferation, significantly increases, while the expression of MMP-1, MMP-3, and MMP-12 decreases [22,23].

We found that after low-dose ALA-PDT was applied to photoaging HDFs, the expression levels of Nrf2, TGF-β1, HO-1, p-ERK and collagen were significantly increased, while those of MMP-9 were decreased. It may be that low-dose photodynamic activation of Nrf2 stimulates antioxidant processes in cells. Other studies have also found that anti-photoaging may be related to activation of antioxidant pathways such as the Nrf2 pathway, upregulation of downstream antioxidant enzyme expression, reductions in ROS, inhibition of lipid peroxidation, reductions in lipid peroxide formation, and protection of cells from damage [24]. Young performed ALA-PDT treatments on 14 patients with facial solar keratosis, and the histopathology results showed that after treatment, average epidermal thickness and inflammatory infiltration of the dermis were significantly reduced, total collagen content was significantly increased, TGF-β and type II TGF-β receptor levels in the epidermis were elevated, and MMP-1, MMP-3, and MMP-12 expression was reduced [25]. Studies by Saw showed that Nrf2-knockout mice were more susceptible to UV-induced skin inflammatory responses and extracellular matrix damage [26] and demonstrated that Nrf2/ARE is an important pathway regulating the intracellular redox status. Huaping Li found that activation of the Nrf2/ARE pathway could help repair damaged DNA and effectively protect cells from UV-induced photodamage [27]. In our experiment, to elucidate the role of Nrf2 in the effects of PDT on photoaging, we first confirmed that a low dose of ALA-PDT could promote nuclear translocation of Nrf2 and then silenced the expression of the Nrf2 gene. We found that cell antioxidant capacity was significantly reduced and that collagen synthesis was reduced by Nrf2 silencing. Thus, it could be assumed that low-dose ALA-PDT reduced ROS, which in turn induced the dissociation of Nrf2 from Keap1. Free Nrf2 translocated into the nucleus and bound to ARE, which upregulated the expression of SOD, TGF-β1, HO-1, and collagens and downregulated the expression of MMP-9, thereby promoting skin collagen remodeling and reducing oxidative damage in HDFs.

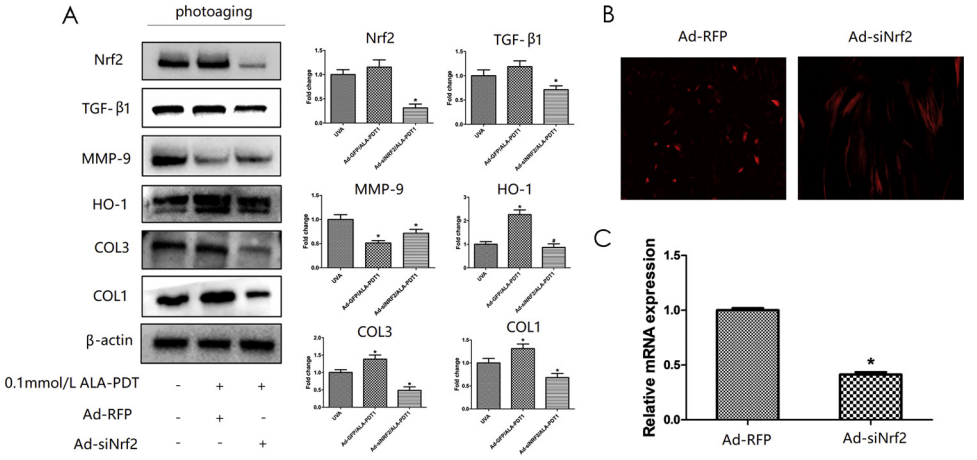

Fig. 5. Effects of Nrf2 knockdown on photoaging HDFs. A: Photoaging HDFs were randomly divided into a UVA group, a low-dose ALA-PDT group infected with Ad-RFP, and a low-dose ALA-PDT group infected with Ad-siNrf2. The expression of Nrf2, TGF-β1, MMP-9, COL1, COL3, HO-1, and β-actin in photoaging HDFs after Nrf2 knockdown by adenovirus infection was confirmed by Western blot analysis. B, C: The Ad-siNrf2 transfection rate was detected by immunofluorescence and qPCR. For COL1, $*p <$ 0.01 versus the other groups. For COL3, $*p <$ 0.01 versus the other groups. For HO-1, $*p <$ 0.01 versus the other groups and $\#p <$ 0.01 versus the Ad-RFP/ALA-PDT1 group. For MMP-9, $*p <$ 0.05 versus the other groups. For Nrf2, $*p <$ 0.01 versus the other groups. For TGF-β1, $*p <$ 0.01 versus the other groups.

5. Conclusion

In conclusion, this study revealed that low-dose ALA-PDT exerts key antiphotoaging effects in HDFs. Nrf2 not only serves as a crucial factor in redox reactions and the effects of photoaging treatment but also regulates the transcription of more than one hundred genes in many pathways in cells, protecting multiple organs and systems. The results of this study will support further elucidation of the role of Nrf2 in the effects of PDT on skin photoaging. In addition, our findings are important for extending the theoretical and experimental basis for the development of PDT indications.

Acknowledgement

This work was supported by National Natural Science Foundation of China grant numbers 81773348, 2017; 81573071, 2015.

References

[1] E. Kohl, et al., Skin ageing, J. Eur. Acad. Dermatol. Venereol. 25 (8) (2011) 873–884, https://doi.org/10.1111/j.1468-3083.2010.03963.x.
[2] M.A. Farage, et al., Intrinsic and extrinsic factors in skin ageing: a review, Int. J. Cosmet. Sci. 30 (2) (2010) 87–95, https://doi.org/10.1111/j.1468-2494.2007.00415.x.
[3] D. Rossetti, et al., A novel anti-ageing mechanism for retinol: induction of dermal elastin synthesis and elastin fibre formation, Int. J. Cosmet. Sci. 33 (1) (2011) 62–69, https://doi.org/10.1111/j.1468-2494.2010.00588.x.
[4] R. Bosch, et al., Mechanisms of photoaging and cutaneous photocarcinogenesis, and photoprotective strategies with phytochemicals, Antioxidants 4 (2) (2015) 248–268, https://doi.org/10.3390/antiox4020248.
[5] K. Kalka, H. Merk, H. Mukhtar, Photodynamic therapy in dermatology, J. Am. Acad. Dermatol. 71 (3) (2000) 389–413, https://doi.org/10.1016/S0190-9622(00)90209-3.
[6] B.C. Alfonso, et al., Protoporphyrin IX-dependent photodynamic production of endogenous ROS stimulates cell proliferation, Eur. J. Cell Biol. 91 (3) (2012) 216–223, https://doi.org/10.1016/j.ejcb.2011.12.001.
[7] J.Y. Hyun, et al., Prolonged activation of ERK contributes to the photorejuvenation effect in photodynamic therapy in human dermal fibroblasts, J. Invest. Dermatol. 133 (9) (2013) 2265–2275, https://doi.org/10.1038/jid.2013.25.
[8] S. Karrer, et al., Photodynamic therapy for skin rejuvenation: review and summary of the literature – results of a consensus conference of an expert group for aesthetic photodynamic therapy, Jddg Journal Der Deutschen Dermatologischen Gesellschaft 11 (2) (2013) 137–148, https://doi.org/10.1111/j.1610-0387.2012.08046.x.
[9] C. Morton, et al., European dermatology Forum guidelines on topical photodynamic therapy, Eur. J. Dermatol. 25 (4) (2015) 296–311, https://doi.org/10.1684/ejd.2015.2570.
[10] M. Schäfer, S. Werner, NRF2 – a regulator of keratinocyte redox signaling, Free Radical Biology & Medicine 88 (Pt B) (2015) 243–252, https://doi.org/10.1016/j.freeradbiomed.
[11] T. Kensler, N.S. Wakabayashi, Cell survival responses to environmental stresses via the Keap1-Nrf2-ARE pathway, Annu. Rev. Pharmacol. Toxicol. 47 (1) (2007) 89–116, https://doi.org/10.1146/annurev.pharmtox.46.120604.141046.
[12] P. Moi, et al., Isolation of NF-E2-related factor 2 (Nrf2), a NF-E2-like basic leucine zipper transcriptional activator that binds to the tandem NF-E2/AP1 repeat of the beta-globin locus control region, Proc. Nat. Acad. Sci. U. S. A. 91 (21) (1994) 9926–9930.
[13] H. Li, et al., Pterostilbene protects against UVB-induced photo-damage through a phosphatidylinositol-3-kinase-dependent Nrf2/ARE pathway in human keratinocytes, Redox Rep. Commun. Free Radical Res. 22 (2) (2017) 1–7, https://doi.org/10.1080/13510002.2017.1329917.
[14] J.J. Wu, et al., Enzyme digestion to isolate and culture human scalp dermal papilla cells: a more efficient method, *Archives of Dermatological Research. Dermatol. Res.* 297 (2) (2005) 60–67, https://doi.org/10.1007/s00403-005-0554-z.
[15] D.C. Florence, et al., UV, stress and aging, Dermato-endocrinology 4 (3) (2012) 236–240, https://doi.org/10.4161/derm.23652.
[16] B. Orit, et al., UV irradiation increases ROS production via PKC delta signaling in primary murine fibroblasts, J. Cell. Biochem. 105 (1) (2010) 194–207, https://doi.org/10.1002/jcb.21817.
[17] H. Mukhtar, Photochemo prevention of ultraviolet B signaling and photocarcinogenesis, Mutat. Res. 571 (1) (2005) 153–173, https://doi.org/10.1016/j.mrfmmm.2004.07.019.
[18] H. Li, et al., Pterostilbene protects against UVB-induced photo-damage through a phosphatidylinositol-3-kinase-dependent Nrf2/ARE pathway in human keratinocytes, Redox Report Communications in Free Radical Research 22 (2) (2017) 1, https://doi.org/10.1080/13510002.2017.1329917.
[19] P. Fonda-Pascual, et al., In situ production of ROS in the skin by photodynamic therapy as a powerful tool in clinical dermatology, Methods 109 (2016) 190–202, https://doi.org/10.1016/j.ymeth.2016.07.008.
[20] H. Masaki, Role of antioxidants in the skin: anti-aging effects, J. Dermatol. Sci. 58 (2) (2010) 85–90, https://doi.org/10.1016/j.jdermsci.2010.03.003.
[21] J.S. Orringer, et al., Molecular effects of photodynamic therapy for photoaging, Arch. Dermatol. 144 (10) (2008) 1296–1302, https://doi.org/10.1001/archderm.144.10.1296.
[22] R. Lubart, et al., A reasonable mechanism for visible light-induced skin rejuvenation, Lasers Med. Sci. 22 (1) (2007) 1–3, https://doi.org/10.1007/s10103-006-0406-x.
[23] M.Y. Park, et al., Photorejuvenation induced by 5-aminolevulinic acid photodynamic therapy in patients with actinic keratosis: a histologic analysis, J. Am. Acad. Dermatol. 62 (1) (2010) 85–95, https://doi.org/10.1016/j.jaad.2009.06.025.
[24] M.C. Issa, et al., Photorejuvenation with topical methyl aminolevulinate and red light: a randomized, prospective, clinical, histopathologic, and morphometric study, Dermatol. Surg. 36 (1) (2010) 39–48, https://doi.org/10.1111/j.1524-4725.2009.01385.x.
[25] P.M. Young, et al., Photorejuvenation induced by 5-aminolevulinic acid photodynamic therapy in patients with actinic keratosis: a histologic analysis, J. Am. Acad. Dermatol. 62 (1) (2010) 85–95, https://doi.org/10.1016/j.jaad.2009.06.025.
[26] C.L. Saw, et al., Nrf2 null enhances UVB-induced skin inflammation and extracellular matrix damages, Cell & Bioscience 4 (1) (2014) 39, https://doi.org/10.1186/2045-3701-4-39.
[27] H. Li, et al., Lycium barbarum polysaccharide protects human keratinocytes against UVB-induced photo-damage, Free Radic. Res. Commun. 51 (2) (2017) 200–210, https://doi.org/10.1080/10715762.2017.1294755.